Review of third and next generation synchrotron light sources

2005 J. Phys. B: At. Mol. Opt. Phys. 38 S773

(http://iopscience.iop.org/0953-4075/38/9/022)

INSTITUTE OF PHYSICS PUBLISHING JOURNAL OF PHYSICS B: ATOMIC, MOLECULAR AND OPTICAL PHYSICS

J. Phys. B: At. Mol. Opt. Phys. **38** (2005) S773–S797 doi:10.1088/0953-4075/38/9/022

Review of third and next generation synchrotron light sources

Donald H Bilderback[1], **Pascal Elleaume**[2] **and Edgar Weckert**[3]

[1] Cornell High Energy Synchrotron Source and the School of Applied and Engineering Physics, 281 Wilson Laboratory, Cornell University, Ithaca, NY 14853, USA
[2] European Synchrotron Radiation Facility, BP 220, F-38053 Grenoble Cedex, France
[3] HASYLAB at Deutsches Elektronen-Synchrotron (DESY), Notkestrasse 85, D-22603 Hamburg, Germany

E-mail: dhb2@cornell.edu

Received 20 January 2005, in final form 17 March 2005
Published 25 April 2005
Online at stacks.iop.org/JPhysB/38/S773

Abstract

Synchrotron radiation (SR) is having a very large impact on interdisciplinary science and has been tremendously successful with the arrival of third generation synchrotron x-ray sources. But the revolution in x-ray science is still gaining momentum. Even though new storage rings are currently under construction, even more advanced rings are under design (PETRA III and the ultra high energy x-ray source) and the uses of linacs (energy recovery linac, x-ray free electron laser) can take us further into the future, to provide the unique synchrotron light that is so highly prized for today's studies in science in such fields as materials science, physics, chemistry and biology, for example. All these machines are highly reliant upon the consequences of Einstein's special theory of relativity. The consequences of relativity account for the small opening angle of synchrotron radiation in the forward direction and the increasing mass an electron gains as it is accelerated to high energy. These are familiar results to every synchrotron scientist. In this paper we outline not only the origins of SR but discuss how Einstein's strong character and his intuition and excellence have not only marked the physics of the 20th century but provide the foundation for continuing accelerator developments into the 21st century.

(Some figures in this article are in colour only in the electronic version)

1. Introduction to synchrotron light sources

To date there exist more than 50 synchrotron radiation sources in operation in the world serving many areas of science ranging from chemistry, biology, physics, material science, medicine to industrial applications. Three generations of sources have been used since the

early times. The third generation sources started operation in the early 1990s. The 'know how' in the development of these sources was initially derived from the experience gained in the early construction of high-energy particle accelerators that started essentially after World War II. These first generation machines were built in order to understand the fundamental laws of matter and particle interactions. Several generations of scientists and engineers from all over the world have participated in this endeavour. The beam dynamics and design of many components constituting these particle accelerators can be traced back to Maxwell's equations, and three names immediately come to mind who pioneered the concepts and the physical understanding required to build these machines, namely J C Maxwell, H A Lorentz and A Einstein.

1.1. The pioneering concepts of Maxwell, Lorentz and Einstein

Modern high-energy accelerators reach electron energies in the GeV (TeV) range for electrons (protons). At such energies, the electrons (protons) are said to be ultra-relativistic. Indeed the electron energy E of a particle of mass m travelling with a velocity v is expressed using the very famous formula first derived in 1905 by A Einstein (Einstein 1905a).

$$E = \frac{mc^2}{\sqrt{1 - \frac{v^2}{c^2}}} = \gamma mc^2 \tag{1}$$

where c is the speed of light and γ is the Einstein relativistic factor. There are two important limits. One is the classical limit where $v \ll c$ corresponding to γ slightly higher than 1 and results in the classical approximation of the energy being the sum of the rest energy and kinetic energy:

$$E = mc^2 + \tfrac{1}{2}mv^2 + \cdots. \tag{2}$$

The other limit is the ultra-relativistic limit where v is close to c (slightly below) with $\gamma \gg 1$.

A 1 GeV electron whose rest mass is 0.5 MeV has a relativistic factor $\gamma = 1000/0.5 = 2000$ which corresponds to a velocity $v/c \simeq 1 - (1/2\gamma^2) = 1 - (1/8)10^{-6}$. In other words, the velocity of a 0.1, 1 or 10 GeV electron is not very different from the speed of light. In this limit, the energy simply defines how close the velocity is to that of the velocity of light. This property, which was anticipated in the special relativity theory proposed by Einstein in 1905, has very deep consequences in the engineering of high-energy particle accelerators. For electrons, the transition energy mc^2 is 512 keV, while for protons it is around 940 MeV. It is known from the Lorentz force that to accelerate some charged particles, an electric field is required since a magnetic field only bends the trajectory. Unfortunately, above a few MeV of acceleration by a static electric field, one faces a major engineering difficulty, that of arcing and breakdown in the high voltage stages. To circumvent this difficulty, engineers have developed a radio frequency (RF) type of acceleration in which the electric fields are not static but oscillate at some frequency. Thus much higher accelerating fields are allowed before breakdown occurs. As a result, RF accelerators are much more economical than electrostatic accelerators.

There have been many different types of RF accelerators among which the most well known are the cyclotrons, synchrocyclotrons, betatrons, linear accelerators and synchrotrons. One of the most successful types of modern high-energy RF accelerators is the synchrotron. One can view a synchrotron as a sequence of magnets that force the trajectory of electrons (or protons) into a closed loop. At one or a few places along the loop, the particles pass through a cavity resonating at a particular frequency of the RF field. A highly resonating cavity generates a large accelerating electric field by means of RF radiation delivered by a

transmitter device of modest power. Because the electrons are ultra-relativistic, their speed is not very different from the speed of light and the time it takes for them to make one turn in the loop is almost independent of their energy if the perimeter of the loop is kept constant. If such a time is an exact integer of the RF period, then the electrons enter the cavity with the same phase on every turn. Depending on this phase they can be repetitively accelerated (or decelerated). As the electron energy increases following successive paths through a RF cavity, the efficiency of the magnets to bend the electron trajectory decreases (proportional to $1/\gamma$ according to the relativistic form of the Lorentz force). It is therefore a necessity to follow the acceleration process by increasing the magnetic field in all magnets in order to maintain a constant perimeter of the loop during the energy ramp cycle. The highest energy reachable is defined by the size of the loop and the highest magnetic field achievable. We have just described the principle of the synchrotron accelerator whose operation is possible because of the invariance of the velocity on the energy as predicted by Einstein.

The success of the synchrotron type of accelerator is also based on other engineering constraints. A machine with constant circumference allows the use of fixed-frequency RF accelerating fields which are economically generated from reasonably powered transmitters when connected to highly resonating cavities of narrow bandwidth. In modern language, the loop consisting of magnets is called a magnetic lattice. The lattice consists of a number of bending magnets with uniform field which bend the trajectory as well as a number of magnetic focusing elements which confine (or focus) the particles around a pre-selected trajectory. Such magnetic focusing elements are called quadrupole magnets which focus the electron beam by using field gradients which bend the charged particle according to their initial position. These magnetic elements are analogous to transparent lenses for visible light where the lenses deflect the angle of light rays depending on their position of entry into the lens.

1.2. General remarks about synchrotron radiation

At this stage, one must discuss synchrotron radiation. By the end of the 19th century, it was understood by a few prominent physicists that any charge which is submitted to an acceleration must radiate some electromagnetic radiation and therefore lose energy. Such radiation is called bremsstrahlung when the accelerating field is electric. It is called synchrotron radiation when the accelerating field is magnetic in origin. The rate of energy loss by synchrotron radiation is important for high-energy particles and scales proportionally to $B^2\gamma^2$ where B is the magnetic field. Since protons are 1840 times heavier than electrons, it requires a much higher energy (γmc^2) for a proton beam to produce the same radiation as an electron beam. As a result, all proton accelerators produce negligible synchrotron radiation and SR is essentially observed only in sufficiently high-energy electron (positron) accelerators. In the 1960s, as higher energy electron synchrotrons were being produced for the research in high-energy physics, the characteristics of synchrotron radiation were well understood theoretically as well as experimentally. Before further developing the properties of synchrotron radiation, it is important to note that from the point of view of accelerator engineering, synchrotron radiation has been somewhat of a nuisance. The total synchrotron radiation power produced grows rapidly with the electron energy. It reaches 1 MW for the 6 GeV, 200 mA electron beam of the European Synchrotron Radiation Facility (ESRF) which requires 2 MW of electricity just to generate the RF field and drive it into the beam through the resonating cavities.

As discussed earlier, the electron energy is ramped in a synchrotron. This is undesirable for a light source where experiments need long periods of steady beam. As a result, present day synchrotron facilities are built around a special fixed-energy synchrotron machine called

a storage ring which is optimally engineered to recirculate the beam for as many turns as is possible. If the chambers hosting the electron beam are sufficiently well evacuated, the lifetime of the beam in a storage ring is typically from 5 to 100 h.

The enormous synchrotron radiation power involved in a circular electron accelerator operating above 100 GeV leads accelerator builders to highly optimized RF accelerating structures in which the acceleration is performed in a multi-kilometre long straight line i.e. linear accelerators that do not involve bending. We are touching here upon the design work of the next International Linear Collider whose technology will also be used for the future single-pass x-ray free electron laser (XFEL), an emerging new ultra-brilliant source of ultra-short duration x-ray radiation (see the companion XFEL paper in this volume by Feldhaus *et al* (2005)).

1.3. Properties of undulator radiation

Let us now concentrate on the properties of synchrotron radiation. The characteristics of such radiation are very precisely derived from the modern form of Maxwell's equations by means of the so-called retarded field, also called the Liénard-Wiechert potentials. The first detailed theoretical investigations of the properties of synchrotron radiation were attributed to Ivanenko and Pomeranchuk (1944), Ivanenko and Sokolov (1948), and Schwinger (1949). Nevertheless, a number of the properties of SR can be traced to the ultra-relativistic nature of the electrons and can be derived from special relativity only through a sequence of Lorentz transformations of the position and the electromagnetic field. Incidentally, Einstein was not very much aware of Lorentz's work in the 19th century and he re-derived these transformations as needed for his theory of relativity.

The most important source of modern third generation light sources is the so-called undulator. An undulator is a periodic magnetic structure typically several metres long which creates a sinusoidal magnetic field along the path of an electron with a spatial period λ_0 and a peak magnetic field $\widehat{B}$. The field is perpendicular to the direction of propagation of the electron.

Let us now consider the spatially oscillating magnetic field of an undulator whose expression in the observer K' frame is given by

$$\vec{E}' = 0 \qquad \vec{B}' = \left(0, \widehat{B}\cos\left(2\pi\frac{z'}{\lambda_0}\right), 0\right) \tag{3}$$

where Oz' is parallel to the electron velocity v. By Lorentz transforming the coordinate z' and the field $\vec{B}'$ into the electron frame, one obtains (see Jackson (1967)):

$$\vec{E} = \gamma\vec{\beta}\times\vec{B}' \qquad \vec{B} = \gamma\vec{B}' - \frac{\gamma^2}{\gamma+1}\vec{\beta}(\vec{\beta}\vec{B}') \qquad \vec{B}' = \left(0, \widehat{B}\cos\left(\frac{2\gamma\pi}{\lambda_0}(\beta ct + z)\right), 0\right) \tag{4}$$

where $\vec{\beta} = v/c$ is the electron velocity in units of the light velocity. For an ultra-relativistic electron, it is easily derived from equation (4) that $\vec{\beta}$, $\vec{E}$, $\vec{B}$ are all perpendicular to each other and that $E = cB = \gamma c\hat{B}\cos((2\gamma\pi/\lambda_0)(z+ct))$. In other words, the undulator magnetic field, seen in the moving electron frame, is transformed into a plane wave of electromagnetic field of frequency $\gamma(c/\lambda_0)$. This field forces the electron into an oscillation and as a result of the associated acceleration, some radiation is produced. If the field is not too strong, the radiation is 'Thomson scattered' at the same frequency. Let the 4-momentum of the back-scattered photon into the direction of the electron be $P_\mu = (p_t,\ p_x,\ p_y,\ p_z) = (\gamma(hc/\lambda_0),\ 0,\ 0,\ \gamma(hc/\lambda_0))$. Transforming to the observer frame K' as in (3), one obtains the 4-momentum in the

ultra-relativistic limit from a Lorentz transformation:

$$P'_\mu = \begin{pmatrix} \gamma & 0 & 0 & \beta\gamma \\ 0 & 1 & 0 & 0 \\ 0 & 0 & 1 & 0 \\ \beta\gamma & 0 & 0 & \gamma \end{pmatrix} \begin{pmatrix} \gamma hc/\lambda_0 \\ 0 \\ 0 \\ \gamma hc/\lambda_0 \end{pmatrix} = (\beta+1)\gamma^2 \begin{pmatrix} hc/\lambda_0 \\ 0 \\ 0 \\ hc/\lambda_0 \end{pmatrix} \simeq 2\gamma^2 \begin{pmatrix} hc/\lambda_0 \\ 0 \\ 0 \\ hc/\lambda_0 \end{pmatrix}. \tag{5}$$

In other words, the wavelength of the synchrotron radiation observed on-axis of an undulator is equal to the spatial period λ_0 divided by $2\gamma^2$. A 20 mm period undulator injected with a 6 GeV ($\gamma \sim 12\,000$) electron beam produces a synchrotron radiation wavelength of 0.058 nm which falls in the hard x-ray range. The Thomson scattering in the electron frame is very slightly directional and the radiation is produced in all directions. Let us consider a photon with frequency ν emitted along the vertical direction, whose 4-momentum is $P_\mu = ((h\nu/c),\ 0,\ (h\nu/c),\ 0)$. In the observer frame the associated four-momentum is derived from (5) as $P'_\mu = (\gamma(h\nu/c),\ 0,\ (h\nu/c),\ \beta\gamma(h\nu/c))$. Clearly the photon is not travelling anymore along the vertical but it has a velocity component along the velocity of the electron. It makes an angle θ with respect to the velocity of the electron which can be expressed as

$$\tan\theta = \frac{p'_y}{p'_z} = \frac{1}{\beta\gamma}. \tag{6}$$

For ultra-relativistic particles ($\beta \approx 1, \gamma \gg 1$), the angle is very small. This is known as the contraction of the angle. Most of the photons of the synchrotron radiation are emitted preferentially along the velocity of the electron in a small cone of emission angle $\theta \simeq 1/\gamma$. Some assumptions have been made so far. In particular, the field of the undulator in the electron frame has been assumed to be weak. A stronger field forces the electron motion to oscillate not only at the frequency $\gamma c/\lambda_0$ but also at all its harmonics $n\gamma c/\lambda_0$ where n is an integer number. An exact derivation of the wavelength, λ, of undulator emission gives

$$\lambda = \frac{\lambda_0}{2n\gamma^2}\left(1 + \frac{K^2}{2} + \gamma^2\theta^2\right) \tag{7}$$

where the dimensionless deflection parameter K is equal to $e\hat{B}\lambda_0/2\pi mc$, and n is the integer number originating from the frequency multiplication induced by the very large electric field in the electron frame. Equation (7) is a fundamental and most general expression which determines the wavelength of the synchrotron radiation produced by relativistic electrons in an undulator. As seen from the application side in a synchrotron facility, it relates the wavelength produced, λ, to the electron energy γ and the undulator field parameters λ_0 and $\hat{B}$. To our knowledge, this analysis was clearly not done by Einstein, but to perform such a derivation, one essentially needed the understanding of spatial and electromagnetic field transformations from one frame to the other set by the theory of relativity and its associated Lorentz transformations.

1.4. Einstein's quantum mechanics contributions are important in synchrotron radiation production

Einstein is not only known as the father of the theory of relativity but he is also recognized as a major contributor to the development of quantum mechanics. In one of his famous papers published in 1905, he explained how to use the constant h (introduced by M Planck several years before) in order to quantize the energy exchange of a photon with an atom or a lattice in a solid providing an elegant explanation of the observed energy threshold in the photoelectric effect (Einstein 1905b). In doing so he is recognized as one of the fathers of the theory of quanta which later was called 'quantum mechanics' (even though he did not fully accept the

Copenhagen interpretation and considered quantum mechanics as an incomplete theory). In this respect it is important to keep in mind that synchrotron radiation is not emitted continuously as it appears from Maxwell's equations and the retarded potentials, but it is emitted in discrete quanta. In other words, electrons emit photons of random energy at random times following a distribution that is in agreement with the predictions from Maxwell's equations. As a result, the energy and momentum quanta fluctuate randomly with time. This type of 'shot noise' induced by the quantum nature of the photon emission accumulates like Brownian motion (Einstein 1905c) and has the very important consequence that the steady-state beam size, beam divergence as well as the energy spread of the electron in a synchrotron are not zero, but are finite with Gaussian distributions (as can be anticipated from the central limit theorem when many independent random variables are added).

Of particular importance for the third generation of sources is the emittance, ε_x, of the beam in the horizontal plane. The emittance is proportional to the surface occupied by the electron beam in the two-dimensional horizontal phase space ($x, x' = \mathrm{d}x/\mathrm{d}s$, where s is a longitudinal coordinate along the main electron velocity). In undulators, the main radiation source of third-generation machines, ε_x, is approximately equal to the product of the RMS horizontal beam size, σ_x, times the RMS horizontal beam divergence, σ'_x. The precise computation of the emittance in a storage ring is given by the following expression (Sands 1971):

$$\varepsilon_x = \frac{55}{64\pi\sqrt{3}}\frac{h}{mc}\gamma^2\vartheta^3\Gamma. \tag{8}$$

The magnet lattice of the storage ring is typically made of a series of identical bending magnets between which special gradient magnets called quadrupole magnets focus the beam. ϑ is the deviation angle of every individual bending magnet, and Γ is a dimensionless parameter defining how optimized the lattice is to generate some small emittance. Importantly, the Planck constant, h, appears in the expression of the emittance confirming the quantum origin of the finite emittance. The dominant contribution to the vertical emittance is not the direct shot noise induced by the emission of quanta but rather the residual coupling of the horizontal to vertical motions, whose expression is

$$\varepsilon_y = \kappa\varepsilon_x \tag{9}$$

where κ is a so-called coupling coefficient of the order of 0.1 to 1% depending only on the fine tuning of the magnets of the lattice. As discussed earlier, the acceleration process only takes place if the electrons are injected into the RF cavities with correct phase with respect to the accelerating RF field. Indeed, as a result of this type of RF acceleration, the electrons are forced to gather longitudinally into bunches spaced at the RF wavelength along the circumference while progressing almost at the speed of light. The longitudinal bunch length of a storage ring is typically a few tens of ps. Its finite size as well as the electron energy spread within a bunch are also determined by the shot noise of the emission process and are quantities that explicitly depend upon Planck's constant.

Third generation synchrotron sources are typically large scale facilities whose figures of merit are multiple. Nevertheless, one of them called brilliance (or equivalently brightness) is of particular importance. The brilliance is defined as the number of photons emitted per second, per photon energy bandwidth, per solid angle and per unit source size. The brilliance of the radiation produced by an undulator is related to the flux and the horizontal (vertical) emittances ε_x (ε_y) as

$$\text{brilliance}[\text{ph s}^{-1}\,(0.1\%)^{-1}\,\text{mm}^{-2}\,\text{mrad}^{-2}] = \frac{\text{flux}}{(2\pi)^2\varepsilon_x\varepsilon_y} = \frac{\text{flux}}{(2\pi)^2\kappa\,\varepsilon_x^2} \tag{10}$$

where the flux is linear in the ring current, I, the number of periods of the undulator field is N_{und}, and $Q_n(K)$ is a dimensionless function which grows with the undulator deflection parameter and depends on the harmonic number, n (as defined in (7)):

$$\mathrm{flux}[\mathrm{ph\ s}^{-1}\ (0.1\%)^{-1}] \propto I N_{\mathrm{und}} Q_n(K). \tag{11}$$

'Brilliance' is important for several reasons. It determines how efficiently an intense flux of photons can be refocused to a small spot size and a small divergence. It is largely invariant during transport (both by electron and optical channels) assuming that the optical components making the transport lines have no aberration. It scales as the ring current (which contributes to the total flux) as well as being inversely proportional to the horizontal and vertical emittances. Thus to maximize the brilliance, the horizontal and vertical emittances must be made as small as possible.

2. Scientific achievements based on research carried out at synchrotron radiation sources

The unique properties of synchrotron radiation (SR) such as wide-energy tunability, high brilliance, extreme collimation, polarization and time structure have enabled a number of new and important techniques since the early days of their use in the 1960s. However, the greatest leap forward occurred in the early 1990s as soon as the first third generation source became available providing extremely brilliant beams in the 100 nm to 1 μm size range. The SR community now numbers in excess of 20 000 individuals (Barletta and Winick 2003). There is not enough space by far in this section to account for all achievements in SR-based research, but an attempt is made to selectively highlight work in some fields such as structural biology, materials science and condensed-matter physics.

2.1. Structural biology

During the last 15–20 years structural biology became a success story of its own with a dramatic increase of knowledge about living organisms on the level of cells as well as at the molecular level. SR has played an extremely important role in this field since the MAD/SAD methods (Hendrickson 1991) to solve unknown crystal structures require a tunable x-ray source. The crystal structure of very large macromolecular complexes could only be solved with the availability of very brilliant SR photons. Examples are the structure of the ribosome (Schlünzen *et al* 2000, Wimberly *et al* 2000, Ban *et al* 2000) and of large viruses (e.g., Grimes *et al* 1998) for which data sets were collected at almost every SR source around the world. These are just two examples and there are many more important structures that help us to understand how biological processes work on a molecular scale such as in studying the interaction of antibiotics with the ribosome (Harms *et al* 2003). At present we know the structure of many—but by far not of all—proteins (mostly soluble) at a molecular to atomic level and we know the structure of cells to much lower resolution. The challenge for the future will be (i) to bridge this gap in resolution from a whole cell to the individual proteins and macromolecular complexes and (ii) to develop methods for the solution of insoluble proteins such as membranes. (A few membrane protein structures have been solved such as that of K-channels leading to the Nobel Prize in Chemistry to Rob MacKinnon in 2003 (Doyle *et al* 1998).) It is expected that SR sources again will play a key role in these efforts.

Another challenge is to understand how proteins and macromolecular complexes work in detail. One very powerful tool in this context is time-resolved studies exploiting the pulsed structure of SR as it has been demonstrated in several cases (e.g. Schotte *et al* 2003). Though

already possible at present, time-resolved studies will certainly obtain an additional boost as soon as shorter duration XFEL and ERL radiation sources become available.

2.2. Materials science

One of the key questions in materials science is to derive macroscopic properties from microscopic structure. There are many established techniques to determine microscopic structure using visible light, electrons or other scanning probes. However, if information on volume properties such as texture and strain in polycrystalline samples have to be investigated, the penetration properties of x-rays are essential. The very collimated and highly energetic SR beams available at e.g. ESRF, APS and SPring8 enable techniques to study all grains and their properties in the interior of a polycrystalline sample with micrometre resolution (Poulsen *et al* 2001, Larson *et al* 2002) even *in situ* under deformation (Margulies *et al* 2001) or during recrystallization (Offermann *et al* 2002). The high brilliance of third generation SR sources in combination with fast detectors allows *in situ* and time-resolved studies that were unthinkable even 10 years ago. An example in this field is the time-resolved radiography of metal foam formation (Banhardt 2001). The coherence properties of these sources enable totally new techniques for imaging bulk low-Z samples or materials with similar absorption by phase contrast imaging, radiography (Gureyev *et al* 1999) and phase contrast micro-tomography (Cloetens *et al* 1999). The low emittance of third generation synchrotron sources provide ideal conditions for microfocus applications thus enabling the study of extremely small samples or regions. For instance, the structure of spider silk was recently investigated by small and wide angle scattering (Riekel *et al* 1999), and local strain measurements have been obtained on a 100 nm length scale in semiconductor devices (Di Fonzo *et al* 2000).

2.3. Condensed-matter physics

Condensed-matter physics is a very wide field and SR-related techniques have always been on the forefront of this physics research area. The available space allows only a few selected examples. The tendency in magnetic storage devices for years is towards higher information density. Continued development requires a profound understanding of magnetism on the nanometre length scale. Circular polarized soft x-rays play a prominent role at this research frontier and, if coherent, they can even be used to directly image magnetic domains by holographic techniques (Eisebitt *et al* 2004). X-ray magnetic dichroism (XMCD) near absorption edges was exploited in the late 1980s to investigate magnetic materials (Schütz *et al* 1988) with elemental selectivity. Since then, XMCD has become one of the standard techniques for the investigation of magnetism because modern SR sources are able to deliver radiation with a very high degree of circular polarization. The high quality of the beams even allowed the discovery of significantly smaller effects such as the natural x-ray circular dichroism of non-centrosymmetric organic compounds (Alagna *et al* 1998).

Nuclear resonant scattering is another one of the techniques that benefits greatly from the new high-brilliance SR sources. Small sample regions can be probed in combination with state-of-the-art focusing techniques. The magnetic spin structure has been imaged in a thin film containing a probe layer of ^{57}Fe atoms (Röhlsberger *et al* 2002).

The properties of matter in the vicinity of surfaces and interfaces are interesting for a number of reasons. Vacuum/air-matter interfaces have been studied for a long time. However, the very collimated hard x-ray beams now available allow x-rays to penetrate even through a bulk layer of lower-Z material to study its interface to a higher-Z layer. Most of these experiments are carried out under grazing incidence conditions where the interface

is illuminated through the optically denser medium (vacuum/air or low-Z material) under a very small angle (in the milliradian range). An example from this field is the investigation of the liquid lead–silicon interface, revealing a five-fold short range order of lead in proximity to the silicon surface (Reichert *et al* 2000). In another example, the accurate geometric structure of an Al_2O_3 oxide layer on a NiAl alloy was determined with implications as to how this type of layer can serve as a template for model catalysts, tunnelling barriers in electronic devices or a model corrosion-resistant layer (Stierle *et al* 2004).

The transverse coherence lengths of ESRF, APS and SPring8 in the x-ray regime are several micrometres in the horizontal and more than 100 μm in the vertical direction. This makes possible the imaging of non-translation periodic objects—thus opening up a totally new method of lensless imaging at very high spatial resolution. The reconstruction of the corresponding object is straightforward (Miao *et al* 1998) if the resulting continuous diffraction pattern is sufficiently over sampled. First experiments have been carried out in order to retrieve the shape of nano crystals (Robinson *et al* 2001) and of synthetic test patterns (Miao *et al* 1999).

So far we have mainly discussed experiments aimed at obtaining the static structure or properties. In recent years, however, powerful new techniques have been established to investigate dynamic properties as well. Inelastic x-ray scattering (IXS) is, meanwhile, a well-established technique for samples where inelastic neutron scattering is not feasible. One important field is the dynamics of liquids and glasses (Sette *et al* 1998, Sinn *et al* 2003, Ishikawa *et al* 2004). Another application has been the determination of the sound velocity of iron at 110 GPa combining high resolution IXS with microfocusing and extreme condition sample environment (Fiquet *et al* 2001). These results also have implications for geophysics.

2.4. A comparison of synchrotron radiation source parameters

Unfortunately this overview has to remain incomplete with a number of fields left out such as chemistry, absorption spectroscopy, micro-fluorescence analysis, etc which also benefit greatly from very small beams, medical applications, geological and environmental science. In all these fields the higher quality of the beams at third generation SR sources has generated new interesting techniques and exciting science follows. It is an easy extrapolation that the improvement in any one of the critical source parameters such as average or peak brilliance, coherence length and pulse duration will provide the means for new techniques helping us to even further improve our knowledge about the material world. Thus we envision synchrotron radiation sources with even further enhanced capabilities.

The next sections describe some of the most promising directions of these future light sources: storage rings at intermediate energy, the ultimate hard x-ray storage-ring light source, and then we describe even longer range opportunities on how the limits to storage-rings can further be overcome with linac-based sources such as an energy recovery linac.

3. Intermediate energy light sources

3.1. Progress in undulator technology makes intermediate energy light sources attractive

While synchrotron radiation covers a wide range of the wavelength spectrum, the highly brilliant undulator emission is only accessible over a narrower range (about a single decade) which depends essentially on the electron energy (as defined in equation (7)) and the capability to produce a high field for a short period set by the undulator technology. In the 1990s, three high energy facilities optimized to generate brilliant undulator radiation in the hard x-range (1–20 keV) were built and commissioned. These are the ESRF, the APS and SPring8 and

Table 1. The most important parameters (energy, current, etc) of many high and intermediate energy synchrotron light sources world-wide are compared in decreasing energy order.

Name	Location	Energy (GeV)	Perimeter (m)	Current (mA)	Emittance (nm rad)	Number of straights
SPRING-8	Japan	8	1436	100	3	48
APS	US	7	1060	100	3	40
ESRF	France	6	844	200	3.8	32
PLS	Korea	2.5	281	180	12	12
ANKA	Germany	2.5	240	110	70	8
SLS	Switzerland	2.4	240	400	5	12
ELETTRA	Italy	2–2.4	260	320	7	12
Nano-Hana	Japan	2	102	300	70	8
ALS	US	1.9	197	400	6.8	12
BESSY-II	Germany	1.7–1.9	240	270	5.2	16

are large capacity sources with 30–50 undulator beamlines each. Table 1 presents a brief list of the most important parameters of these sources compared to others presently in operation world-wide. The electron energy is an essential parameter since it determines the size and the cost of the facility as well as how short a wavelength can be produced from undulators.

There is a gap in the distribution of electron energy between the three hard (higher energy) x-ray sources and the other facilities of much lower cost and size and for which undulators cover the VUV or the soft x-ray regime. The hard x-ray facilities need a large number of such undulators and, as a result, undulator technology has improved and dramatically matured. Undulators were initially thought to be only usable on harmonics 1 to 3 because of the reduction of flux and brilliance owing to very small magnetic field errors. Thus phase or spectrum shimming has been successfully developed (Chavanne and Elleaume 1995) to overcome this limitation. It has been shown now that much higher harmonic radiation can be generated with high flux and brilliance.

Further progress in undulator technology has been made by operating the devices at very small magnetic gap. In this respect, it has become possible to operate undulators with a magnetic gap of around 5 mm or less by placing the permanent magnets which generate the undulator field inside the vacuum chamber itself.

The concept is not new but the engineering was first developed on a large scale at the SPring8 source (Hara *et al* 1998). Small undulator gaps allow small periods and therefore increase the energy of the undulator emission (equation (7)). The consequence is that the same photon energy can be obtained from a lower energy electron beam but with a higher harmonic of the undulator emission and/or by using a shorter period, λ_0.

3.2. Parameters of intermediate energy sources

The electron energy is an essential factor which drives the field of the magnets of the lattice, the size of the lattice and its associated infrastructure and, therefore, the overall cost of the facility. The new trend is thus to build lower cost, intermediate energy light sources that are available in many local regions. The parameters of these sources are given in table 2 and generally feature an electron energy of 3 GeV with a capacity of 12 to 24 undulator beamlines. These sources will complement the higher energy facilities and possibly compete with them. For example, SOLEIL and DIAMOND are expecting a low emittance of around 3 nm rad coupled with a large capacity of 24 beamlines. A symposium took place in Shanghai,

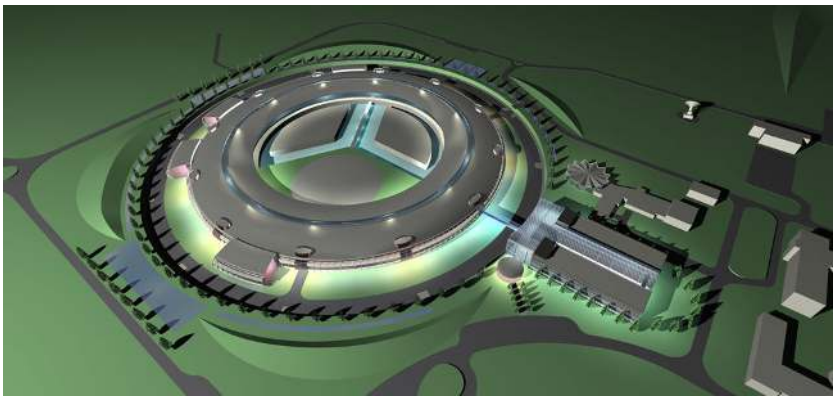

Figure 1. Artist's rendition of the DIAMOND light source under construction in the UK.

Table 2. Intermediate energy sources recently commissioned or under commissioning or construction (by decreasing order of commissioning date).

Name	Location	Energy (GeV)	Perimeter (m)	Current (mA)	Emittance (nm rad)	Number of straights
SPEAR3	US	3	240	500	18	18
CLS	Canada	2.9	171	500	18	12
SOLEIL	France	2.85	354	500	3.1	16 + 8
DIAMOND	UK	3	560	300	2.7	24
Australian Synchrotron	Australia	3	216	200	8.6	14
ALBA	Spain	3	268.8	250	3.7	4 + 8 + 12
SSRF	China	3.5	396	300	4.8	20

Table 3. New projects of intermediate-energy sources presently under study or waiting for approval. We note that the NSLS II and MAX-IV rings are aggressively optimized for a high current and very low emittance of the electron beam.

Name	Location	Energy (GeV)	Perimeter (m)	Current (mA)	Emittance (nm rad)	Number of straights
NSLS II	US	3	620	500	1.5	24
MAX-IV	Sweden	3	285	500	1.2	12
SESAME	Jordan	2.5	120	400	27	16
TLS-II	Taiwan	3	240	400	10	16
CANDLE	Armenia	3	224	350	8.4	16
Indus-II	India	2.5	173	300	58	8

China (Shanghai Symposium 2001) reviewing the intermediate-energy synchrotron sources. A summary of the design issues and performance values has been written (Corbett and Rabedeau 2003). Figure 1 presents an artist's rendition of the 3 GeV DIAMOND facility under construction in the UK.

There are many other ring projects that are under study or are now looking for funding. Their parameters are summarized in table 3.

Current lists of SR facilities are kept by a number of groups including the SSRL group (Winick and Nuhn 2004). The websites are really essential for staying up to date in this field.

Table 4. Parameters of the ultimate high-energy x-ray source compared to those of the present third generation high-energy sources.

Name	Place	Energy (GeV)	Perimeter (m)	Current (mA)	Emittance (nm rad)	Number of straights
UHXS	–	7	2200	500	0.2	48
SPRING8	Japan	8	1436	100	3	48
APS	US	7	1060	100	3	40
ESRF	France	6	844	200	3.8	32

4. Ultimate high-energy x-ray source

The three hard x-ray facilities were commissioned in the 1990s and a number of intermediate energy sources are under construction around the world. All are pushing for further technological innovations with the highest hard x-ray performances still belonging to the highest energy facilities.

But now is the time to ask ourselves an important question. How could we best use the lessons learned in the past 15 years to design and build an ultimate high-energy x-ray source (UHXS)? Several directions have been identified.

4.1. Design considerations and spectral curves of future UHXS source

In 2000, a study was performed at ESRF on the design of such a source (Ropert *et al* 2000). What is proposed is a large capacity source of 40 to 50 undulator beamlines with optimal flux and brilliance in the 0.5–500 keV range with an emphasis in the 10–20 keV range. This may be obtained by simultaneously running a high current of 500 mA and a very small electron beam emittance of around 0.2 nm rad in the horizontal plane and smaller than 0.01 nm rad in the vertical plane. The horizontal emittance is 40–80 times smaller, and the current is 2.5–5 times larger than those achieved in presently operating synchrotron radiation facilities of similar energy. The operation at a 500 mA current requires 7 MW of radio frequency power to be delivered to the beam through a series of radio frequency cavities, thus producing a total accelerating voltage around 14 MV over the circumference of the machine. These voltage and power levels are necessary to compensate for the energy and power loss by the electrons due to synchrotron radiation emission in the bending magnets and undulators. At this high current, some instabilities can occur through the interaction of the beam with the so-called higher order resonant mode of the radio frequency cavities (HOM). Recent development in the engineering of radio frequency cavities make the operation at such a high current possible by either using superconducting technology (already in use in the newly built 3 GeV sources) or by using conventional room temperature copper cavities equipped with heavy dampers for the HOMs (as developed for the high current electron *B*-factories at SLAC and KEK). An electron energy of 7 GeV has been selected for the UHXS which is a compromise between lifetime, beam stability and cost. The main parameters of this source are given in table 4.

4.2. Challenges of heat loads and lattice design

The beamlines are equipped with mirrors to refocus the beam onto the samples and monochromators to select a narrow slice of the spectrum. One of the major issues in the operation of such a facility is the extreme heat load on the mirrors and monochromators. An undulator beam from this source will produce a power of 50 kW and a power density close to

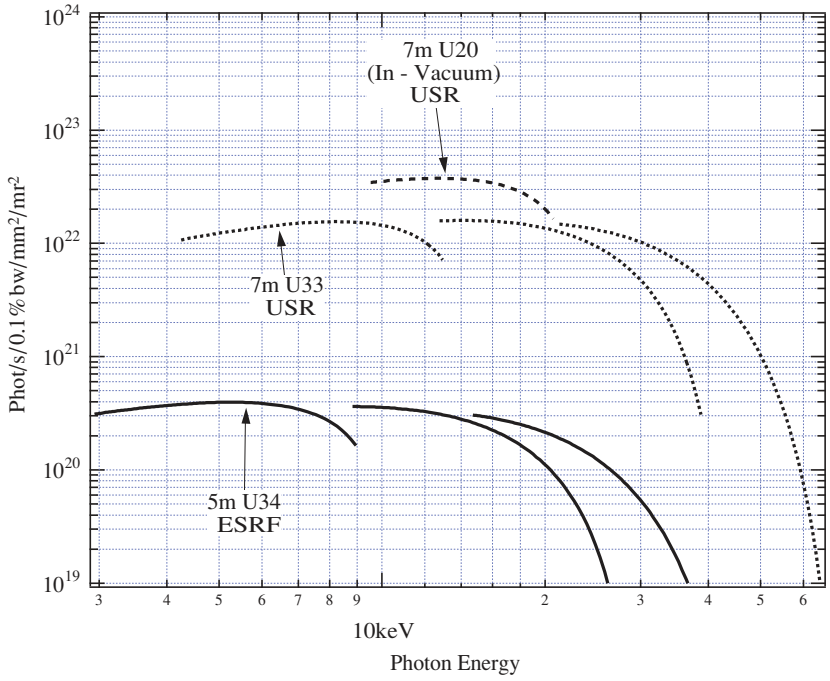

Figure 2. Brilliance versus photon energy of the ultimate high-energy x-ray source (UHXS or USR) compared to those achieved on a typical undulator at the ESRF facility.

1 kW mm^{-2} at a distance of 40 m from the undulator. To maintain a narrow energy resolution, most monochromators are likely to be made of silicon crystals cooled by liquid nitrogen (a technology already in use in the hard x-ray facilities). Diamond crystals may also be used with room temperature water cooling. A narrow slit (typically 0.5 $\times$ 0.5 mm^2) will be placed in front of the crystal. The slit reduces the power to 250 W while transmitting most of the flux available on the harmonics of the undulator spectrum. The lower the electron beam emittance, the smaller the aperture of the slits (for the same flux collection) and therefore the lower the transmitted power. The achievement of the small emittance is thus essential and is a major challenge. In addition, the lower the emittance, the longer is the transverse coherence length obtained from the undulator. (The radiation produced can be just as coherent as a laser beam.) Thus very low emittance opens the door to a number of new experiments which make use of the coherence (speckle, holography, etc). While a 7 GeV ring could be built with a circumference of 500 m but with a rather large emittance around 20 nm rad, the achievement of a 0.2 nm rad emittance requires a much larger perimeter of 2200 m. The reduction of the emittance is obtained by segmenting the bending magnets into a large number of short units separated by quadrupole magnets which refocus the beam from one bending magnet to the other. The space required by these quadrupoles is the reason for the increase of the circumference. Such a ring would contain 160 bending magnets and 720 quadrupole magnets to be compared to 64 and 320, respectively, for the ESRF. Indeed the increased size of the circumference is one of the prices to pay for the low emittance. Figure 2 shows the expected brilliance from a conventional fully tunable undulator installed on such a source compared to the brilliance produced by an ESRF undulator.

There are several other challenges besides the heat load and lattice design. In storage rings, electrons make transverse horizontal and vertical oscillations around a reference orbit. However electrons executing a large oscillation may not follow stable trajectories and can ultimately be lost on a wall of the vacuum chamber. To avoid such loss, the number of oscillations per circumference (called the tune number) must be carefully selected. In addition, the spread of tune must be controlled within narrow limits. The strong quadrupoles used between the bending magnets have a focusing strength that varies in inverse proportion to the electron energy. As a result they induce a so-called chromatic aberration with the tune varying from one electron to the next according to its energy. For the beam to be stable, the chromatic aberrations must be compensated. This is done with special magnets called sextupoles. Roughly speaking, sextupoles can be understood as focusing elements whose focal strength varies with the injection point. However, sextupoles induce another type of aberration which makes large transverse oscillations unstable. This results in a reduction of the transverse aperture (dynamic aperture) below that due to the vacuum chamber wall. The design and location of the sextupoles must be carefully selected in order to correct the chromatic aberration while keeping a large dynamic aperture. This is a non-trivial task because of the large sextupolar strength required. The small emittance and high current results in a high density of the beam. As a result of the high density, a large number of collisions take place every second between electrons within a single bunch. The colliding electrons may lose or gain energy to the point that their associated trajectory in the ring becomes unstable. The lifetime of the stored electron beam is therefore reduced by this intra-beam scattering. Contrary to modern hard x-ray sources which have a lifetime in the range of 50–100 h, the UHXS will have a significantly shorter lifetime of around 5 to 10 h. The short-beam lifetime will induce a beam orbit drift through the variation of power load from synchrotron radiation during the decay of the beam current. The remedy might simply be to inject one or a few mA of current every 5 or 10 min using a continuously running injector system. It is likely that such a source will require a number of slow and fast active stabilization feedback systems to prevent the onset of transverse and longitudinal instabilities and to maintain the stability of the centre of gravity of the beam to a fraction of the beam size. Such feedback systems have already been implemented on a number of rings, and the associated technology is considered mature. Other challenges in the design of such a source include tight mechanical tolerances in the machining of magnets, precise alignment and sensitivity to ground vibrations.

4.3. Challenges of enlarging the dynamic aperture and operating with damping wigglers

One of the most important design challenges of such a lattice involves the enlargement of the dynamic aperture in order to reach a value sufficient for injection. In this respect, we mention another promising alternative to the UHXS which is based on damping wigglers. Such a facility would be simply derived from a double bend achromat lattice (two bending magnets between undulators) similar to those at the ESRF, APS or SPring8 and be built around low-field bending magnets and a number of damping wigglers (a special type of undulator device with a long period (200–500 mm) and a high field (1–2 T)) and produce brilliant undulator-type radiation only at low energy (as derived from equation (7)). The wigglers would be a few metres long each but their accumulated length along the circumference could reach several hundred metres. Preliminary investigations indicate that such a source could reach a similar low emittance and would be of similar circumference to the UHXS or possibly even smaller. Such a facility would require more RF power and be quite innovative in the sense that most of the synchrotron radiation would be produced at a few locations inside the damping wigglers rather than in the bending magnets. One of the challenges will be in handling the high

power generated by these wigglers. On the other hand, the achievement of a large enough dynamic aperture appears easy. The concept of such damping wigglers is not new and has been employed already on the LEP and DAFNE storage rings. Damping wigglers are also planned for the PETRA III upgrade and are incorporated in the designs of all the lepton damping rings required for the various projects of high-energy linear colliders.

5. Description of PETRA III

5.1. Introduction

The 4.5 GeV storage ring DORIS III in Hamburg at present serves as the main source for synchrotron radiation (SR) at DESY with 9 wiggler beamlines and more than 30 bending magnet stations. Two additional experimental stations are operated at an undulator beamline at the PETRA II storage ring (12 GeV) running in parasitic mode. The photon energies provided for experiments range from the VUV to several hundred keV. Being a second generation source, the wigglers and bending magnets of DORIS III provide high flux in quite large beams. While these parameters are ideal for the investigation of large samples, extremely small samples can only be investigated by strongly focused and therefore divergent beams. Due to the large source size of DORIS III, it is nearly impossible to generate a focused beam in the micrometre range or below. In this respect modern third generation sources are much more capable.

DESY's longer term perspective is the European x-ray free electron laser project besides the VUV-FEL starting user operation in 2005 (see companion article by Feldhaus *et al* (2005)). The lasers will provide a transverse coherent beam with peak brilliances several orders of magnitude higher than any present synchrotron radiation source. It is DESY's intention, however, to also provide photons of very high brilliance from storage rings to the user community in addition to laser radiation in the future. For this reason the 2304 m circumference PETRA storage ring will be transformed into a third generation SR source for hard x-rays from year 2007 onwards.

5.2. Reconstruction of PETRA

The reconstruction of PETRA into a third generation SR source is described in detail in a Technical Design Report (Balewski *et al* 2004). PETRA was designed as an electron–positron collider for energies up to 23.5 GeV in the late 1970s and was the first machine to discover the gluon. At present PETRA is used as a 12 GeV lepton and 40 GeV proton pre-accelerator for the HERA high-energy proton–lepton collider experiments. The present PETRA lattice is of the FODO type (a sequence of focusing and defocusing quadrupoles separated by non-focusing elements such as bending magnets or drift spaces) and consists of octants (each with radii of 254.7 m) that are connected by four 64.8 m 'short' and four 108 m 'long' straight sections. The reconstruction of PETRA will include the total rebuilding of one octant of the present storage ring to provide the electron beam optics for nine straight sections (23 m long double bend achromat (DBA) cells consisting of two bending magnets and a number of quadrupoles between the straight sections) each providing space for one 5 m long insertion device or two canted 2 m long insertion devices that will be inclined by about 5 mrad towards each other. The latter configuration will result in a beam separation of about 16 cm at the end of the shielding wall enabling independent safety systems and optics for each of the undulator beams. The magnetic lattice of the remaining part of the storage ring will not be changed, however, the parts that will totally be refurbished include the renewal of the vacuum system, wire wound coils for all magnets, cooling system, power supplies, beam

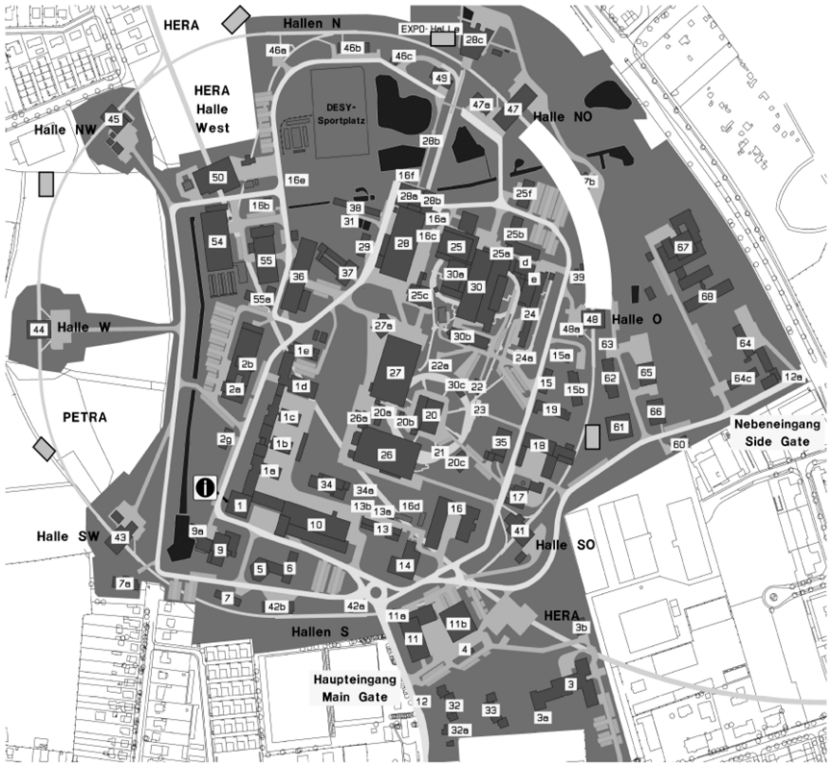

Figure 3. Plan of the DESY site: the position of the new experimental hall is shown in white arc between buildings 47 and 48. Additional beamline buildings are sketched in hatched squares at positions where further undulator beamlines can be placed in future.

diagnostics and beam controls, just to mention the most important items. Figure 3 shows the position of the new experimental hall (288 m long and 32 m wide) on the DESY campus.

Depending on the exact beamline outline (which is still under discussion) about 13 beamlines will be available with independently tunable insertion devices. The length of the first undulator (close to building 47, figure 3) can be up to 20 m. For future upgrades there are two other locations at the PETRA storage ring where such a long undulator can be located. In addition there are further positions in the storage ring for the installation of additional insertion devices that do not need any major change of the magnetic lattice but they would require the construction of new buildings. Thus in total, about 18 insertion device positions are available.

PETRA III will be operated at a particle energy of 6 GeV with an initial current of 100 mA. All components, however, will be designed for a current of at least 200 mA. The proposed upgrade aims for an emittance of 1 nm rad (1% coupling ratio) which will be achieved with 20 damping wigglers (each 4 m long, peak field of 1.52 T, 20 cm period) installed into the free 'long' straight sections of the storage ring. The total power emitted by these damping wigglers will be about 400 kW at 100 mA as compared to the 120 kW emitted from all bending magnets. At present there are no plans to use the radiation emitted from the damping wigglers for experiments. However, some materials science applications in the future might be able to use these large, hard x-ray beams.

The number of bunches in a smooth filling pattern will be between 40 and 960, corresponding to bunch separations of 192 ns to 8 ns, respectively, with lifetimes ranging

Table 5. Overview of typical β-functions, RMS photon source sizes $\sigma_{Tx,y}$ and divergences $\sigma_{Tx',y'}$ for the ID positions at PETRA III. The x (y) direction is horizontal (vertical). The photon source parameters are given for a photon energy of roughly 12 keV.

	β_x (m)	β_y (m)	σ_{Tx} (μm)	σ_{Ty} (μm)	$\sigma_{Tx'}$ (μrad)	$\sigma_{Ty'}$ (μrad)	ID length (m)
Low β	1.3	3	36	6	28	3.7	5
High β	20	2.4	141	5.5	7.7	3.8	5

from 2 to 24 h. The RMS bunch length will be 20 ps. The heat load on the storage ring components as well as on the photon optics has to be kept as constant as possible in order to maintain photon beams of very high stability. For this reason a topping-up mode of operation is envisaged, e.g. the injection of small charges on a time scale of minutes, which will require some refurbishment of components in the DESY pre-accelerator chain for increased reliability.

The maximum beamline length inside the new experimental hall will be about 100 m although some of the beamlines may be extensible to greater than a 300 m length.

5.3. Insertion devices and beam characteristics at PETRA III

A minimum aperture of 7 mm and state-of-the-art vacuum pipe design will allow magnetic gaps of the insertion devices down to 9.5 mm with conventional in-air undulators. While the horizontal emittance $\varepsilon_x = \sigma_x \sigma_x'$ of a storage ring is a constant, the so-called $\beta_{x,y}$-function ($\beta_x = \sigma_x/\sigma_x'$) of the particle beam at the position of the insertion devices can be adjusted to the needs of the experiment. Typical values for β-functions and the related photon source sizes at the envisaged insertion device positions are compiled in table 5.

As at the ESRF, two β-function values will be available that can independently be selected for each straight section. A comparison of these source parameters with those of other high-energy synchrotron radiation sources reveals that there is only a small improvement in the vertical direction towards smaller source sizes and lower divergences at a 12 keV photon energy. However, the benefit of a lower horizontal emittance of 1 nm rad becomes clearly obvious in this direction. At the same photon beam divergence of an ESRF, APS or SPring8 beam, the PETRA III horizontal source size will be about three to four times smaller.

The advantages of a smaller source point for micro- and nano-focusing applications are clear. The transverse coherence length (according to $\xi = \lambda L/(2.35\sigma_{Tx,y})$, with λ the wavelength and L the source-sample distance) calculated from the FWHM of the source sizes will be about 500 μm in the vertical direction for both β-function values. Horizontal coherence lengths of 18 μm and 72 μm will be obtained at 12 keV photon energy for the high and low β-function straight sections, respectively. Thus PETRA III will be a diffraction-limited source up to photon energies of about 10 keV in the vertical direction and up to 100 eV in the horizontal direction.

The brilliance of different undulators for PETRA III is shown in figure 4. These plots were calculated for a 1% coupling ratio. The total coherent flux according to $F_c = B(\lambda/2)^2$ at about 12 keV is 4×10^{10}, 10^{11} and 2.5×10^{11} ph/s/0.1%BW for a 2 m, 5 m and 20 m insertion device, respectively. The advantage of a high-energy storage ring is the considerable flux that these devices can provide for small photon beams even at very high x-ray energies. In figure 5 the photon flux for very hard x-rays through a 1 mm^2 pinhole at 40 m distance from the source is compared for different PETRA insertion devices and some hard x-ray devices from other high-energy SR sources. It becomes clear that at very high x-ray energies at PETRA III, a $K = 7.7$ wiggler device will provide more flux even through a small pinhole than a standard undulator.

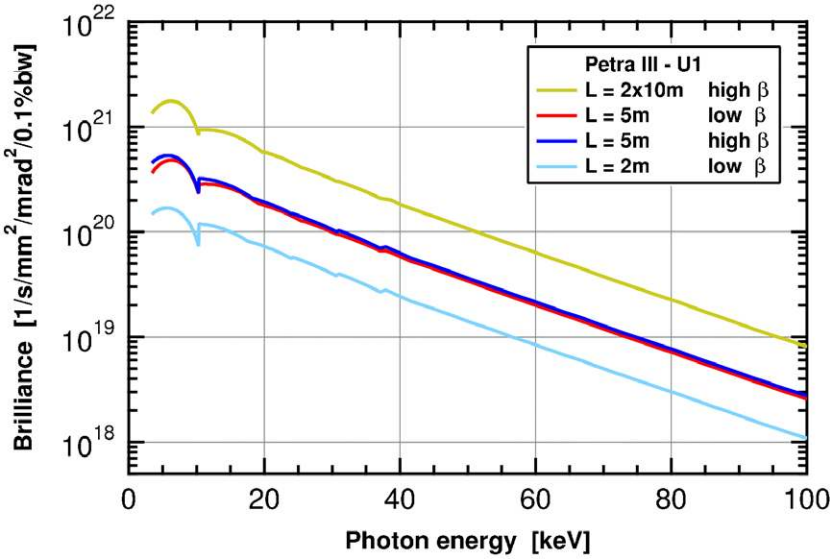

Figure 4. Comparison of the brilliance of typical PETRA III undulators. The calculations assume ideal undulators, e.g. the real brilliances in the higher energy region will generally be slightly smaller. The calculations assume a 1 nm rad emittance, 1% coupling, 6 GeV energy, 100 mA current, a minimum magnetic gap of 9.5 mm, 29 mm magnetic period and $K_{max} = 2.2$. The upper, middle and lower curves correspond to undulator lengths of 2 × 10 m, 5 m and 2 m, respectively. All brilliances and source sizes were calculated using SPECTRA (Tanaka and Kitamura 2003).

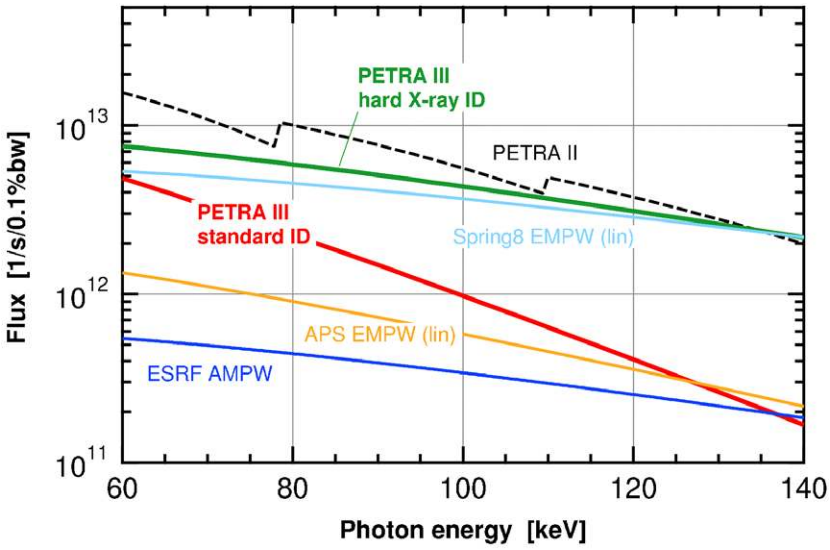

Figure 5. Comparison of the flux through a 1 mm^2 pinhole at a 40 m distance from the source from a standard PETRA III undulator with dedicated high-energy insertion devices from present sources. The PETRA III hard x-ray device is a 5 m $K = 7.7$ wiggler with a 4.9 cm period length. The flux for the present PETRA II undulator operating at 12 GeV was calculated for a pinhole at a 100 m distance.
Note: this comparison is only relevant for apertures <1 mm in size.

In this energy range the performance values shown of the wiggler devices of the other sources depend mainly on the design of the insertion device, the particle energy and current of the storage ring and not on the emittance.

Possible alternative hard x-ray insertion devices are in-vacuum undulators and, as soon as their feasibility has been shown, superconducting (Rossmanith *et al* 2002) and variable period undulators (Shenoy *et al* 2003). A 4 m in-vacuum undulator ($K_{\max} = 2.2$, 23 mm period) at PETRA III will provide almost the same brilliance compared to the standard 5 m insertion device for photon energies below 20 keV and a two to three times higher value above 80 keV. A hypothetical 4 m long superconducting device ($K_{\max} = 2.2$, 15 mm period) will provide a maximum brilliance of 10^{21} at low energies and will be more than an order of magnitude more brilliant in the 80–100 keV range. This, however, assumes that the phase error of the superconducting device can be adjusted to an accuracy comparable to present permanent magnet devices.

There also is a quite strong science case for the VUV and XUV energy range at a high-energy SR source if undulator radiation with a very high degree of circular polarization (from the first undulator harmonic) is needed.

A soft VUV/XUV insertion device at PETRA III will provide more or less the same flux as similar devices at the ESRF, APS and SPring8 but with a brilliance slightly beyond 10^{20} at about a 2 keV photon energy.

5.4. Comparison of PETRA III to other high-energy SR sources and the UHXS

It is commonly accepted practice to use the source brilliance to compare the performance of different synchrotron radiation facilities (equation (10)). Among a number of other parameters, the brilliance of a source depends inversely on the horizontal and vertical emittances of the storage ring. PETRA III with its 1 nm rad horizontal emittance will have a factor 3–4 advantage compared to the ESRF, APS and SPring8 assuming the same horizontal–vertical coupling ratio. For higher photon energies the higher particle energy at APS and especially at SPring8 reduce this factor slightly. In principle the brilliance can nominally be increased further by reducing the coupling ratio, a step which has successfully been applied at the ESRF and SPring8. However, there are only a few experiments that can take advantage of this additional increase, and a lower coupling ratio has a negative influence on the intrinsic Touschek lifetime especially of storage rings with very low emittance (see also section 4). During the last years the ESRF machine group has carried out a study on what could be the ultimate storage ring, the UHXS (see section 4). The UHXS would be a storage ring with about the same circumference as PETRA and an emittance of 0.2 nm rad which is five times lower than the present PETRA III target value. Comparing these numbers, one can consider the PETRA III performance to be almost half way in between the present high-energy storage rings and the UHXS study. In summary, in the foreseeable future, until the UHXS is built, PETRA III is expected to be the lowest emittance storage-ring available for the hard x-ray science community.

6. The energy recovery linac as a next-generation light source

6.1. DC photocathode guns and superconducting RF cavities promise to revolutionize x-ray source construction

Users of synchrotron radiation (SR) are generally interested in improving the qualities of the SR such as high average and peak brilliance, flux, the coherence of the emitted beam, and

in obtaining ultra-short bunch lengths for timing experiments. All of these properties follow from the properties of the emitting electron bunch—a situation that can greatly be improved if we can obtain synchrotron radiation from the 'enhanced electron bunches' circulating in an energy recovery linac (ERL) rather than from electron bunches circulating in storage rings. The technology for storage rings is at the point of diminishing returns as the present technology has been almost fully optimized for light source production after some 40 years of development. The use of huge rings and damping structures (e.g., UHXS and PETRA III (see sections 4 and 5 respectively)) represents the best of the ideas on how to maximize the usefulness of hard SR sources to the limits of today's understanding.

The ERL technology, on the other hand, provides the prospect of orders of magnitude further improvement in critical parameters, and it is still in its infancy in terms of technology development (Gruner and Bilderback 2003). Only recently have the developments in dc photocathode guns and high accelerating gradient superconducting cavities been brought together with a design that promises to revolutionize the way future synchrotron x-ray sources can be constructed. The first practically significant demonstration of an ERL facility was the Infrared Free Electron Laser machine at Jlab (Neil *et al* 2000).

6.2. Machine parameter improvements possible with an ERL

Extraordinary flux can be achieved from an ERL operating at 5.3 GeV, 200 mA and with 25 m long undulators. With very small transverse emittances of 8 pm rad in the high coherence mode, the electron beam cross-sectional area can be made a thousand times smaller than that in the current APS storage ring, thus making a more brilliant x-ray source. And as the transverse beamsize falls to as small as 2 μm RMS in the ERL, it becomes a nearly fully diffraction-limited x-ray source in the hard x-ray regime of 1 Å (12 keV) with more than 3 000 times the coherent flux produced by the APS (figure 6). By making short bunches in a photoinjector, the natural bunch length of 2 ps can further be compressed with bunch compressors to yield pulses shorter than 0.1 ps, several hundred times shorter than the 73 ps long ESRF bunches in a single-bunch mode. More details about the machine and the further spectral curves can be found at the ERL website (Shen 2004a).

6.3. How an ERL machine produces enhanced SR performance

An ERL machine is like a storage ring in that a similar magnet lattice is used to guide electrons around the circumference. As the beam passes through the insertion devices, x-rays are produced. They differ, however, in one very important way. The electrons recirculate many times around a storage ring, whereas in the Cornell ERL design, they make just one pass around the ring. It is this essential difference that leads to the expected enhanced performance.

Assume for the moment that a very bright electron source feeds two machines: one a third generation storage ring and the other an ERL type machine (figure 7). In a storage ring, the injected bunches are generally brought up to full energy by a synchrotron or a linear accelerator and injected into a nearly circular ring where they circulate many times. Within several thousand orbits around the storage ring, the initially small phase-space volume of the bunches expand to fill the larger phase-space volume dictated by the ring lattice and RF system. The ERL, on the other hand, recovers energy and dumps the bunches after one (or at most a few) transits around the machine, before they suffer phase-space expansion. Thus, the bunches that yield the x-rays are small in all three dimensions—yielding a more brilliant, fully transversely coherent source of x-rays with very short bunch lengths! Since the improvements are not factors of 2 or 5 or 10 over storage-ring performance values, but rather factors of

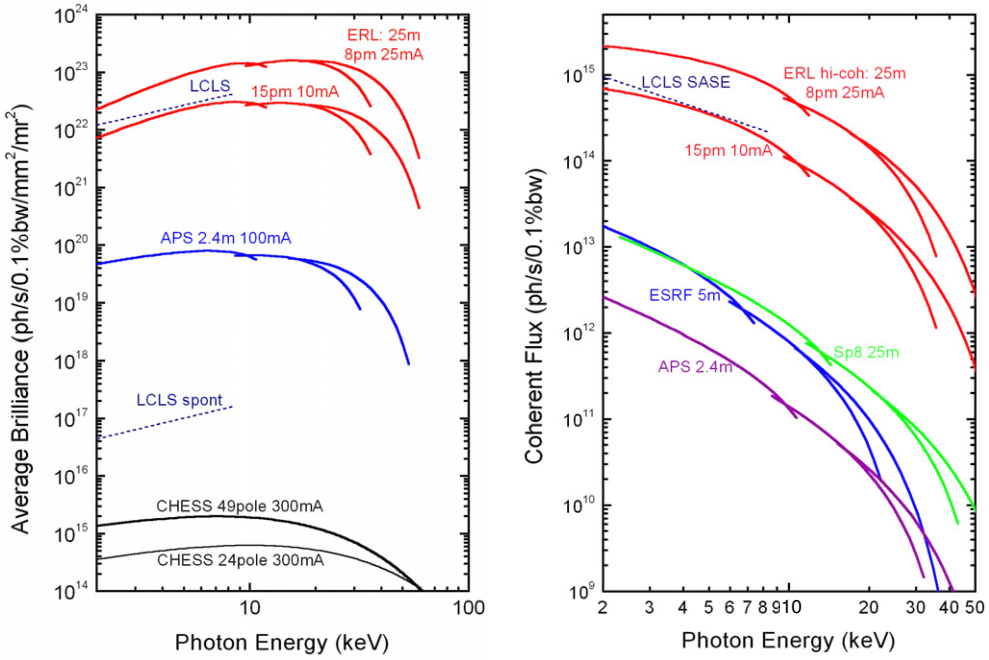

Figure 6. Average brilliance and coherent flux for CHESS, the linac coherent light source, the APS, ESRF and the proposed ERL machine under different operating modes (8 pm, 25 mA hi-coherence mode; 15 pm, 10 mA ultra-fast mode) and 25 m long undulators.

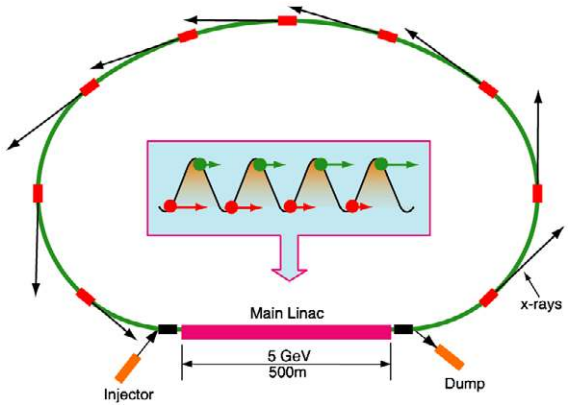

Figure 7. Schematic diagram of an energy recovery linac source of synchrotron radiation. A bright electron source injects electrons at up to a 1.3 GHz rate into a superconducting radio frequency cavity that accelerates electrons to full energy of 5 GeV (the green balls 'surfing' on the crest of the RF travelling wave). They circulate around a return arc producing brilliant x-ray beams in undulators (shown as red rectangles). The circumference of the arc is adjusted so that the path length of the electrons returning to the linac is 180° out of accelerating phase. Thus these returning (red ball) electrons ride in the trough of the RF wave and now give up their energy to the cavity. After being decelerated to low energy they are directed to a beam dump. Each electron makes one trip around the loop and its energy is recycled in the main linac, hence the name, energy recovery linac

hundreds to many thousands, we believe that this machine will be transformational to the way synchrotron science will be accomplished into the next decades after such a source is first demonstrated.

The vision at Cornell University is to construct the key prototype part, the photoinjector, and to test it between 5 MeV and 15 MeV with currents up to 100 mA. We plan to perform additional tests in collaboration with other laboratories to resolve remaining design questions. We then hope to submit a proposal for a full-energy (e.g., 5.3 GeV) ERL proposal as an upgrade to the CESR ring that now powers CHESS. Given adequate funding, we estimate that a full-energy proposal can be submitted by about 2008. Construction of a full-energy upgrade would take about 5 years.

The wonderful part of ERL technology is that it makes a beam that is compatible with all existing experiments that are being done today at storage rings, yet it opens up the possibilities of new types of experiments, particularly in the areas of nano-beams, coherence and ultra-fast science. Therefore all the current x-ray techniques developed at storage rings can immediately be employed and then pushed to further new limits. Below we give several examples of the type of science that could be accomplished on an ERL in biological, materials science and condensed-matter physics areas.

6.4. ERL science examples

Microfabricated flow cells have been developed by the L Pollack group at Cornell where macromolecules in solution fold up when suddenly mixed with a higher pH buffer solution (Russell *et al* 2002). This SAXS experiment was prototyped at CHESS and then taken to the APS where millisecond temporal resolution was achieved. With the smaller, even more intense ERL microbeams, this experiment (which is brilliance limited) can be taken to a microsecond time scale where there is interest to follow the kinetics on an even faster time scale.

We also plan to develop a nanoprobe beamline for material science experiments and will try to see if we can develop optics to make a 1 to 10 nm diameter beamsize in the 1 to 10 keV regime. If optical issues can be resolved satisfactorily (this will require zone plates that are currently beyond the state of the art but might be possible with further R&D), we might be able to focus an x-ray beam onto ultra-small objects and begin x-ray imaging, absorption, holography, etc experiments on single atoms, molecules, clusters and larger nanoparticles (Bilderback and Huang 2004).

Since the ERL will be a diffraction-limited light source, coherent imaging and diffraction experiments from non-periodic structures will be an especially important theme. We should be able to study the structure of non-crystalline materials, frozen biological cells, etc by collecting and analysing coherent diffraction patterns from which we should be able to reconstruct a real-space image. The spatial resolution is expected to be close to atomic resolution for materials samples and of the order of a few nanometres for biological specimens, a limit determined by radiation damage (Shen 2004b). Not having to have a crystalline object will greatly open up the number of samples available for study.

The last example is a pump–probe experiment of J Brock's from Applied Physics at Cornell. By suitably choosing the diffraction geometry and incident energy, x-rays can be scattered in charge density wave (CDW) systems from inner core electrons that are resonant in energy with the Fermi energy. (A CDW is a long wavelength perturbation of a crystalline lattice.) By varying the diffraction conditions, the spatial structure of specific valence electronic states can be explored. A fast femtosecond Ti:sapphire laser with a 78 MHz repetition rate (wavelength of about 800 nm, 0.1 to 1 μJ cm^{-2}) may be used to cyclically pump electrons across the energy gap, suppressing the CDW state. By performing

a pump-probe measurement, the dynamics of excited states becomes accessible. These time constants are expected to vary from femtoseconds to nanoseconds. Since the ERL will have a programmable laser that can pulse x-rays at a variable frequency (up to a maximum frequency of 1.3 GHz, the fundamental RF mode in the linear accelerator), the probe x-ray frequency can be chosen to match the experimental conditions that are needed. From the resonant x-ray scattering information, a time-dependent structural model of how the crystal responds to the pump beam will be obtained—information that is highly desired by solid-state physicists.

Of course, these are just but a few of the 'teasers' of the kind of ultimate science we hope to accomplish with a new ERL source. Since the ERL will genuinely be a 'better light bulb' than existing sources, we can look forward to many creative scientists dreaming up many new applications across the fields of science where the advanced features of the ERL will make a real difference in what can be accomplished. The ERL x-ray source is a very exciting prospect for the future!

7. Perspectives on the future

We are excited that research with synchrotron radiation continues to generate enthusiasm in the broader interdisciplinary science community. Understanding how accelerators and the science experiments best work together continues to be an important theme for optimizing their mutual usefulness to each other. We are hoping that the future SR community will have enough beamtime, research funding and trained manpower to meet the demands at current facilities. This existing base, coupled with the build up of several new projects under design/construction, will continue to expand our scientific horizons in synchrotron radiation research for decades to come.

All of the accelerator operations of our entire synchrotron radiation enterprise depend upon the very foundations that Einstein laid last century in his development of special relativity. We are pleased to recognize, at the century mark, the wonderful impact that the precision control of relativistic electrons has had on our branch of synchrotron science.

Acknowledgments

We thank Professor Dr Horst Schmidt-Böcking for inviting us to contribute this paper and our numerous colleagues who have grown the SR field over the last decades into a large diverse science community. This work is based in part upon research conducted at the ESRF, HASYLAB and the Cornell High Energy Synchrotron Source (CHESS) which is supported by the National Science Foundation and the National Institutes of Health under award DMR-0225180.

References

Alagna L, Prosperi T, Turchini S, Goulon J, Rogalev A, Goulon-Ginet C, Natoli C R, Peacock R D and Stewart B 1998 *Phys. Rev. Lett.* **80** 4799

Balewski K, Brefeld W, Decking W, Franz H, Röhlsberger R and Weckert E (ed) 2004 PETRA III: a low emittance synchrotron radiation source *Technical Design Report* DESY 2004-035 (Online available at http://www-hasylab.desy.de/facility/upgrade/petra_tdr.htm)

Ban N, Nissen P, Hansen J, Moore P B and Seitz T A 2000 *Science* **289** 905–20

Banhardt J, Stanzick H, Helfen L and Baumbach T 2001 *Appl. Phys. Lett.* **78** 1152–4

Barletta W A and Winick H 2003 *Nucl. Instrum. Methods Phys. Res.* A **500** 1–10

Bilderback D H and Huang R 2004 CP705 *Synchrotron Radiation Instrumentation: 8th Int. Conf.* ed T Warwick *et al* (New York: American Institute of Physics) pp 1271–3
Chavanne J and Elleaume P 1995 Undulator and wiggler shimming *Synchrotron Radiat. News* **8** 18–22
Cloetens P, Ludwig W, Baruchel J, van Dyck D, van Landuyt J, Guigay J P and Schlenker M 1999 *Appl. Phys. Lett.* **75** 2912
Corbett J and Rabedeau T 2003 *Nucl. Instrum. Methods* A **500** 11–7
Di Fonzo S, Jark W, Lagomarsino S, Giannini C, De Caro L, Cedola A and Müller M 2000 *Nature* **403** 638–40
Doyle D A, Cabral D M, Pfuetzner R A, Kuo A, Gulbis J M, Cohen S L, Chait B T and MacKinnon R 1998 *Science* **280** 69–77
Einstein A 1905a *Ann. Phys.* **17** 891
Einstein A 1905b *Ann. Phys.* **17** 132
Einstein A 1905c *Ann. Phys.* **17** 549
Eisebitt S, Lüning J, Schlotter W F, Lörgen M, Hellwig O, Eberhardt W and Stöhr J 2004 *Nature* **432** 885
Feldhaus J, Arthur J and Hastings J B 2005 *J. Phys. B: At. Mol. Opt. Phys.* **38** S799
Fiquet G, Badro J, Guyot F, Requardt H and Krisch M 2001 *Science* **291** 468
Grimes J M, Burroughs J N, Gouet P, Diprose J M, Malby R, Zientra S, Mertens P P C and Stuart D I 1998 *Nature* **395** 470–8
Gruner S M and Bilderback D H 2003 *Nucl. Instrum. Methods* A **500** 25–32
Gureyev T E, Raven C, Snigirev A, Snigireva I and Wilkins S W 1999 *J. Phys. D: Appl. Phys.* **32** 563–7
Hara T, Tanaka T, Tanabe T, Marechal X M, Okada S and Kitamura H 1998 *J. Synchrotron Radiat.* **5** 403–5
Harms J M, Bartels H, Schlünzen F and Yonath A 2003 *J. Cell. Sci.* **116** 1391–3
Hendrickson W 1991 *Science* **254** 51–8
Ishikawa D, Inui M, Matsuda K, Tamura K, Tsutsui S and Baron A Q R 2004 *Phys. Rev. Lett.* **93** 097801
Ivanenko D and Pomeranchuk I Ya 1944 *Dokl. Akad. Nauk (USSR)* **44** 343
Ivanenko D and Sokolov A 1948 *Dokl. Akad. Nauk (USSR)* **59** 1551
Jackson J D 1967 *Classical Electrodynamics* (New York: Wiley) chapter 11.10
Larson B C, Yang W, Icr G E, Budai J D and Tischler J Z 2002 *Nature* **415** 887–90
Margulies L, Winther G and Poulsen H F 2001 *Science* **291** 2392–4
Miao J, Sayre D and Chapmann H N 1998 *J. Opt. Soc. Am.* **15** 1662–9
Miao J, Charalambous P, Kirz J and Sayre D 1999 *Nature* **400** 342–3
Neil G R *et al* 2000 *Phys. Rev. Lett.* **84** 662–5
Offermann S E, van Dijk N H, Sietsma J, Grigull S, Lauridsen E M, Margulies L, Poulsen H F, Rekvedt M T and van der Zwaag S 2002 *Science* **298** 1003–5
Poulsen H F, Nielsen S F, Lauridsen E M, Schmidt S, Suter R M, Lienert U, Margulies L, Lorentzen T and Juul Jensen D 2001 *J. Appl. Cryst.* **34** 751
Reichert H, Klein O, Dosch H, Denk M, Honkimäki V, Lippmann T and Reiter G 2000 *Nature* **408** 839
Riekel C, Müller M and Vollrath F 1999 *Macromolecules* **32** 4464–6
Robinson I K, Vartanyants I A, Williams G J, Pfeifer M A and Pitney J A 2001 *Phys. Rev. Lett.* **87** 195505/1–4
Röhlsberger R, Thomas H, Schlage K, Burkel E, Leupold O and Rüffer R 2002 *Phys. Rev. Lett.* **89** 237201
Ropert A, Filhol J M, Elleaume P, Farvacque L, Hardy L, Jacob J and Weinrich U 2000 Towards the ultimate storage ring based light source *EPAC 2000* (Available at http://accelconf.web.cern.ch/accelconf/e00/PAPERS/TUZF101.pdf)
Rossmanith R, Moser H O, Geisler A, Hobll A, Krischel D and Schillo M 2002 *Proc. EPAC Conf. EPAC2002 (Paris)* p 2628
Russell R *et al* 2002 Rapid compaction during RNA folding *Proc. Natl Acad. Sci. USA* **99** 4266–71
Sands M 1970 The physics of electron storage rings: an introduction *Proc. Int. School of Physics Enrico Fermi* p 46 (also available as *SLAC Internal Report 121* November 1970, 172 pp)
Schlünzen F *et al* 2000 *Cell* **102** 615–23
Schotte F, Lim M, Jackson T A, Smirnov A V, Soman J, Olson J S, Phillips G, Wulff M and Anfinrud P A 2003 *Science* **300** 1944–7
Schütz G, Knülle M, Wienke R, Wilhelm W, Wagner W, Kienle P and Frahm R 1988 *Z. Phys. B.: Condens. Matter* **73** 67
Schwinger J 1949 *Phys. Rev.* **75** 1912
Sette F, Krisch M H, Masciovecchio C, Ruocco G and Monaco G 1998 *Science* **280** 1550
Shanghai Symposium 2001 *Proc. Shanghai Symposium on Intermediate Energy Light Sources* (Available at http://ssils.ssrc.ac.cn/)
Shen Q 2004a *Expected Performance of the Proposed Cornell ERL X-Ray Source* file at http://erl.chess.cornell.edu/misc/Shen_Expected_Performance_of_ERL_14April2004.pdf

Shen Q, Bazarov I and Thibault P 2004b *J. Synchrotron Radiat.* **11** 432–8
Shenoy G K, Lewellen J W, Shu D and Vinokurov N A 2003 *J. Synchrotron Radiat.* **10** 2005–213
Sinn H, Glorieux B, Hennet L, Alatas A, Hu M, Alp E E, Bermejo F J, Price D L and Saboungi M L 2003 *Science* **299** 2047
Stierle A, Renner F, Streitel R, Dosch H, Drube W and Cowie B C 2004 *Science* **303** 1652
Tanaka T and Kitamura H 2003 *Program SPECTRA* (Japan: RIKEN Institute for Physical and Chemical Research)
Wimberly B T, Bordersen D E, Clemons W M Jr, Morgan-Warren R I, Carter A P, Vonrhein C, Hartsch T and Ramakrishnan V 2000 *Nature* **407** 327–39
Winick H and Nuhn H D Website of synchrotron resources (present & planned) world-wide can be found at http://www.lightsources.org